Antarctic Science 23(6), 589–596 (2011) © Antarctic Science Ltd 2011 doi:10.1017/S0954102011000411

Interannual variability of net community production and air-sea CO_2 flux in a naturally iron fertilized region of the Southern Ocean (Kerguelen Plateau)

MARIE PAULE JOUANDET[1], STEPHANE BLAIN[2,3], NICOLAS METZL[4] and MATHIEU MONGIN[5]

[1]*Laboratoire d'Océanographie Physique et Biogéochimique, Campus de Luminy, case 901, 13288 Marseille CEDEX 09, France*
[2]*CNRS, UMR7621, LOMIC, Observatoire Océanologique, F-66650 Banyuls-sur-Mer, France*
[3]*UPMC Université Paris 06, UMR 7621, LOMIC, Observatoire Océanologique, F-66650 Banyuls-sur-Mer, France*
[4]*LOCEAN-IPSL, UMR 7159, CNRS, Université P. et M. Curie-Case 100, 4 place Jussieu, F-75252 Paris CEDEX 5, France*
[5]*CSIRO Marine and Atmospheric Research, Hobart, TAS 7001, Australia*
MariePaule.Jouandet@utas.edu.au

Abstract: The interannual variability of net community production (NCP) and air-sea CO_2 flux in a naturally iron fertilized and productive area of the Southern Ocean (Kerguelen plateau) was investigated using a 1D biogeochemical model driven by satellite chlorophyll, sea surface temperature and wind speed data for the 1997–2007 period. The model simulates the low fCO_2 and dissolved inorganic carbon (DIC) measured during summers 2004–05, 2005–06, 2006–07 and the high NCP derived from a seasonal carbon budget in the surface waters of these blooms. Although satellite data show high interannual variability in the dynamics and magnitude of the bloom during the 1997–2007 decade, the simulated interannual variability of the NCP was only ± 14%. This unexpected result could be due to the combined effect of both the duration and the start date of the bloom, the latter determining the depth of the mixed layer used to compute the NCP. In the productive area, the interannual variability of air-sea CO_2 flux (± 13%) was not only driven by the biological effect but also by the solubility effect. Our results contrast with previous studies in the high nutrient, low chlorophyll regions of the Southern Ocean.

Received 28 June 2010, accepted 14 March 2011, first published online 27 June 2011

Key words: Antarctic waters, biogeochemical model, carbon flux

Introduction

Rate of organic matter exported from surface waters in the Southern Ocean removes CO_2 from the atmosphere, thereby influencing the atmospheric CO_2 concentrations. Over the seasonal scale, carbon export can be approximated by net community production (NCP) (rate of organic carbon production in excess of respiration). In the Southern Ocean, the distribution of NCP is characterized by large spatial variability (Karl *et al*. 1991, Bates *et al*. 1998, Rubin *et al*. 1998, Ishii *et al*. 1998, 2002, Cassar *et al*. 2007, Hoppema *et al*. 2007). While the Southern Ocean is the largest high nutrient, low chlorophyll (HNLC) region in the global ocean, high marine productivity does occur during the summer near frontal systems, downstream of islands and over shallow topography in the Antarctic Circumpolar Current (Sullivan *et al*. 1993, Moore & Abbott 2002, Tyrrell *et al*. 2005).

The Kerguelen Ocean and Plateau compared Study (KEOPS, January–February 2005) aimed to compare the high productive area localized over the Kerguelen plateau with the surrounding HNLC waters (Fig. 1). The bloom over the Kerguelen plateau was sustained by an increased supply of iron and major nutrients (Blain *et al*. 2007). The core of the bloom was characterized by low sea surface CO_2 fugacity in seawater ($fCO_2 < 320$ µatm), representing a large CO_2 sink for the atmosphere ($\Delta fCO_2 = -50$ µatm) and is in contrast with the near equilibrium conditions observed outside the bloom. The NCP, derived from a seasonal budget of dissolved inorganic carbon (DIC) (Jouandet *et al*. 2008) was roughly three times higher in the core of the bloom (6.6 ± 2.2 mol m^{-2}) than outside (1.9 ± 0.4 mol m^{-2}) and similar to the NCP in other productive areas of the Southern Ocean (Karl *et al*. 1991, Ishii *et al*. 1998, Sweeney *et al*. 2000).

In this study we combined new field observations collected during three successive summers (2005–07) that include remote sensed chlorophyll, temperature and wind (1997–2007) data and a two-box biogeochemical model to explore the impact of the interannual variability of the bloom, specifically its duration and timing, on the magnitude of the NCP. We also investigated the effect of biology and temperature interannual variability on the CO_2 sink (ΔF_{atm}) over the 1997–2007 period.

Materials and methods

Computational method to simulate NCP and fCO_2

For the bloom duration defined as the period with chlorophyll a (chl *a*) > 0.3 mg m^{-3} (Table I), the seasonal

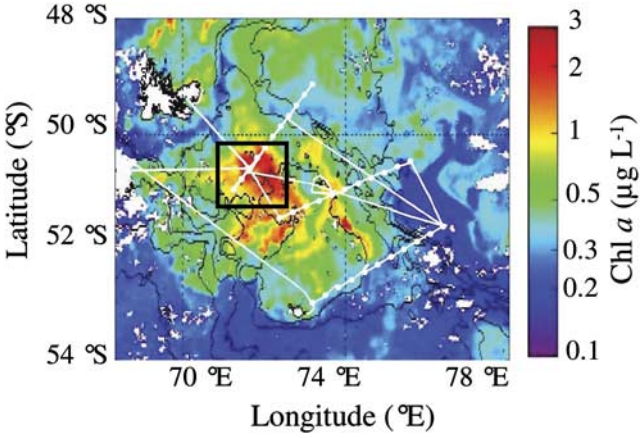

Fig. 1. Distribution of chl *a* over the Kerguelen plateau during the KEOPS cruise, as estimated by satellite remote sensing. A black square delimits the core of the bloom. A white line represents the KEOPS cruise track (January–February 2005).

NCP and integrated air-sea CO_2 flux (ΔF_{atm}) were computed, as follow:

$$NCP = \int (\delta DIC/\delta t)_{bio}\, MLD(t)\, dt \quad (1)$$

$$\Delta F_{atm} = \int F_{atm}(t)\, dt = \int k \cdot k_0 \cdot (fCO_{2air} - fCO_{2sea})\, dt, \quad (2)$$

where $(\delta DIC/\delta t)_{bio}$ is the daily variation of DIC due to the biological activity in the mixed layer (ML), k_0 is the solubility (Weiss 1974) and k the gas exchange coefficient. The air-sea gas exchange process sensitivity to k was tested using different parameterizations (Wanninkhof *et al*. 1992, Nightingale *et al*. 2000, Ho *et al*. 2006). The interannual variability of ΔF_{atm} did not change according to the k parameterization. We present here results using the Ho *et al*. (2006) parameterization, determined for the Southern Ocean. Atmospheric fCO_2 (fCO_{2air}) was estimated using the atmospheric CO_2 concentrations from the OISO (Ocean Indian Service Observation) records compiled in the south Indian Ocean region since 1998 (Metzl 2009). $(\delta DIC/\delta t)_{bio}$ and fCO_{2sea} seasonal cycles were simulated using a new version of the 1D biogeochemical model previously described in details in Louanchi *et al*. (1996) and Jabaud-Jan *et al*. (2004). The initial model independently took into account four processes that control the seasonal variations of fCO_2 in the surface waters: the air-sea CO_2 exchange, the thermodynamics (solubility), the biological activity and vertical mixing (entrainment) between surface and subsurface waters.

This model was applied and adapted to the Kerguelen bloom by adding turbulent vertical mixing processes, and changing the biogeochemical module. The silicic acid limitation pointed out by Mosseri *et al*. (2008) in the studied region was taken into account. $(\delta DIC/\delta t)_{bio}$ was then derived from the $Si(OH)_4$ variation due to the biological activity $(\delta Si/\delta t)_{bio}$, using the ratio of biogenic silica (BSi) vs

Table I. Comparison of the bloom characteristics (duration, starting date, magnitude). The bloom duration is defined as the period when the chl *a* concentrations were above 0.3 mg m^{-3}. The beginning of the cycle is on 1 October for all years.

Season	1997–98	1998–99	1999–2000	2000–01	2001–02	2002–03	2003–04	2004–05	2005–06	2006–07
Duration (days)	148	164	164	140	152	168	120	136	144	120
Start of the bloom	1–8 Nov	17–24 Nov	24–31 Oct	17–24 Nov	9–16 Nov	24–31 Oct	17–24 Nov	1–8 Nov	17–24 Nov	9–16 Nov
End of the bloom	22–29 Mar	1–8 May	7–14 Apr	7–14 Apr	7–14 Apr	7–14 Apr	22–29 Mar	14–21 Mar	30 Mar–7 Apr	22–29 Mar
Chl *a* (1st peak) (mg m^{-3})	1.08	3.02	1.76	1.29	1.94	2.42	1.57	1.2	4.21	2.28
Week	17–24 Nov	9–16 Jan	17–24 Nov	19–26 Dec	19–26 Dec	17–24 Nov	19–26 Dec	25 Nov–2Dec	27 Dec–1 Jan	11–18 Dec
Chl *a* (2nd peak) (mg m^{-3})	1.81	2.78	1.54	2.05	1.58	1.08	1.4	1.15	2.35	0.9
Week	17–24 Jan	10–17 Feb	11–18 Dec	1–8 Jan	25 Jan–2 Feb	17–24 Jan	17–24 Jan	9–16 Jan	9–16 Jan	9–16 Jan

https://doi.org/10.1017/S0954102011000411 Published online by Cambridge University Press

Table II. Parameters used to constrain the model for all the simulations.

	Model	*In situ*
R_{resp}	0.45	–
$R_{\rho POC/\rho BSi}$ [1]	5.2	–
$R_{BSi/chl\ a}$ (mol g^{-1})[2]	3.7	3.3 ± 0.4
$K_{Si(OH)4}$ (μM)[2]	4	4–11[3]
μ_{max} (d^{-1})[2]	0.45	0.1–0.3[3]

[1] Obernosterer *et al.* 2008
[2] Mosseri *et al.* 2008
[3] kinetic parameters of the largest size fraction (> 10 μm) which dominated the phytoplankton composition of the bloom

particulate organic carbon (POC) in the organic matter ($R_{\rho POC/\rho BSi}$) and a respiration coefficient (R_{resp}):

$$(\delta DIC/\delta t)_{bio} = (1\text{-}R_{resp})\cdot R_{\rho POC/\rho BSi}\cdot(\delta Si/\delta t)_{bio} \quad (3)$$

$(\delta Si/\delta t)_{bio}$ was computed from chl *a* changes (δchl *a*) using the silicon uptake kinetic parameters ($K_{Si(OH)4}$, μ_{max}) and the ratio BSi/chl *a* ($R_{BSi/chl\ a}$):

$$(\delta Si/\delta t)_{bio} = \mu_{max}[Si(OH)_4]/([Si(OH]_4+K_{Si(OH)4})\cdot\delta chl\,a. \quad (4)$$

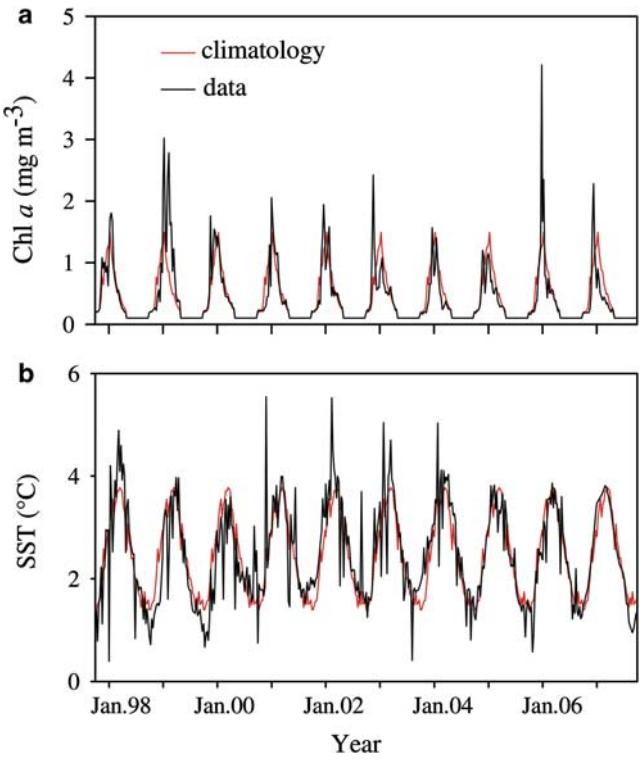

Fig. 2. Temporal variations of **a.** chl *a*, and **b.** sea surface temperature (SST) from the 1 October 1997 until the 1 October 2007, in the core of the bloom over the Kerguelen plateau. Chlorophyll *a* and SST were averaged for periods of eight days, in the area of 51 ± 1°S by 72.6 ± 1.0°E (this is representative of the core of the bloom south-east of the Iles Kerguelen). Red lines denote the seasonal climatology.

All parameters (R_{resp}, $R_{\rho POC/\rho BSi}$, $K_{Si(OH)4}$, μ_{max}, $R_{BSi/chl\ a}$) were constant through the seasons (Table II). This assumption is discussed later. The first step of the model implementation was to constrain $K_{Si(OH)4}$, μ_{max}, $R_{BSi/chl\ a}$ to reproduce the low $Si(OH)_4$ concentration measured in January 2005, during KEOPS. $R_{BSi/chl\ a}$ and $K_{Si(OH)4}$ were fixed to the extreme values (Table II) measured for the largest size fraction, which dominated the composition of the phytoplankton bloom (Mosseri *et al.* 2008). The maximum growth rate, which was the most sensitive parameter of the model, was $\mu_{max} = 0.45$ d^{-1}, and was higher than the measured values (Mosseri *et al.* 2008) but still lower than values used in previous models for the Southern Ocean (Pondaven *et al.* 2000, Fasham *et al.* 2006). $R_{\rho POC/\rho BSi}$ was fixed using a $R_{resp} = 0.45$ (Obernosterer *et al.* 2008). $R_{\rho POC/\rho BSi}$ was then fixed to 5.2, which is in the range of experimental values (Mosseri *et al.* 2008) and lower than the usual ratio BSi/C of Brzezinski (1985).

This set of parameters was then able to simulate NCP derived from the DIC seasonal budget for the 2004–05 bloom ($NCP_{cal} = 6.6 \pm 2.2$ mol m^{-2}; Jouandet *et al.* 2008).

At each time increment (one day) the model also evaluates total alkalinity (TA), and sea surface fCO_2 is computed from DIC and TA. As interannual variability of both sea surface salinity (SSS) and TA is low in this region, we used the same SSS and TA/SSS relations as in previous studies (Jabaud-Jan *et al.* 2004, Metzl *et al.* 2006).

The model was constrained with weekly (rather than monthly as in the original version) sea surface temperature (SST), chl *a* and sea surface wind speed (SSW) to take into account episodic peaks of productivity as seen in the SeaWIFS chl *a* cycles (Fig. 2a) as well as large SST anomalies (Fig. 2b). Chlorophyll *a* and SST were averaged over eight days periods, in a 51 ± 1°S by 72.6 ± 1.0°E area, which represented the core of the bloom south-east of the Iles Kerguelen (Fig. 1). Chlorophyll *a* constrains were provided by the SeaWiFS Project, NASA/Goddard Space

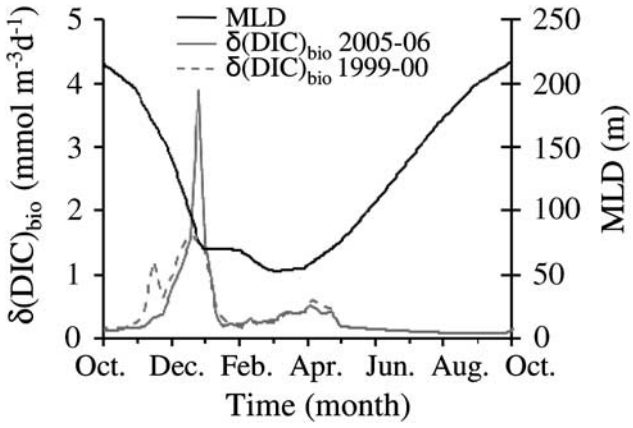

Fig. 3. Seasonal evolution of the mixed layer depth (MLD) (from Metzl *et al.* 2006) and the simulated $(\delta DIC)_{bio}$ for the 1999–2000 and 2005–06 blooms.

https://doi.org/10.1017/S0954102011000411 Published online by Cambridge University Press

Table III. Comparison between seasonal observed and simulated biogeochemical properties in surface waters. Numbers in italic indicate simulated values obtained using the 1D biogeochemical model at the date of measurements. The range of each simulated parameter for January is given in brackets.

	Jan 2005	Jan 2006	Jan 2007
$Si(OH)_4$ (μmol kg^{-1})	2 ± 1	3 ± 1	17 ± 2
Mod. $Si(OH)_4$	*2*	*1*	*7*
	(*1.25–8.32*)	(*0.7–3.4*)	(*1.7–7.4*)
DIC (μmol kg^{-1})	2107 ± 3	2118 ± 1	2119 ± 7
Mod. DIC	*2110*	*2104*	*2113*
	(*2110–2120*)	(*2104–2112*)	(*2109–2115*)
fCO_2 (μatm)	318 ± 2	318 ± 2	315 ± 2
Mod. fCO_2	*304*	*285*	*309*
	(*304–318*)	(*280–300*)	(*300–315*)
NCP (mol m^{-2})	6.6 ± 2.2	6.3 ± 2.5	6.4 ± 2.6
Mod. NCP	*8.5*	*8.4*	*8.4*

Flight Center and GeoEye (http://oceancolor.gsfc.nasa.gov/cgi/l3, accessed October 2007) and AVHRR SST data (ftp://podaac.jpl.nasa.gov/pub/sea_surface_temperature/avhrr/pathfinder/data_v5/8day, accessed October 2007) both with a 9 km resolution. Sea surface wind speed was derived from the CERSAT products (ftp://ftp.ifremer.fr/ifremer/cersat/products/gridded/mwf-quikscat/data/weekly/, accessed October 2007). The seasonal variation of the mixed layer depth (MLD) follows Metzl *et al.* (2006). The MLD cycle (Fig. 3) is in agreement with the MLD of 70 ± 20 m based on density criteria (mean value of the 40 conductivity, temperature, depth profiles; Jouandet *et al.* 2008) and a residual winter layer of 210 m (depth of the minimum temperature) measured during KEOPS in January 2005.

Initial conditions were the concentrations measured at the depth of minimum temperature of the reference station (50°38'S, 72°05'E) located in the core of the bloom (DIC_{winter} = 2170 μmol kg^{-1} and $Si(OH)_{4winter}$ = 27 μmol kg^{-1}; Jouandet *et al.* 2008). The simulation started on 1 October and ran for one year, thus, hereafter a year is from 1 October of the year *n* until 1 October of the year *n*+1.

Interannual variability of chl a *concentrations and SST during 1997–2007*

Results show strong interannual variability in both the dynamic (duration and timing) and the magnitude (intensity of the peaks) of the bloom (Table I, Fig. 2a). The longest blooms were observed during the 1998–99, 1999–2000 and 2002–03 years with an average duration of 165 ± 2 days. The shortest blooms were in 2003–04 and 2006–07 (duration of 120 days). In 1999–2000 and 2002–03, the spring bloom started 3–4 weeks earlier (last week of October) than other years. All blooms were characterized by two peaks in chl *a*. The first peak occurred in the second half of November (17 November–2 December) in the years 1997–98, 1999–2000, 2002–03 and 2004–05, and one month later (19–31 December) in 2000–01, 2001–02 and 2003–04. In 1998–99 the first peak occurred in early January.

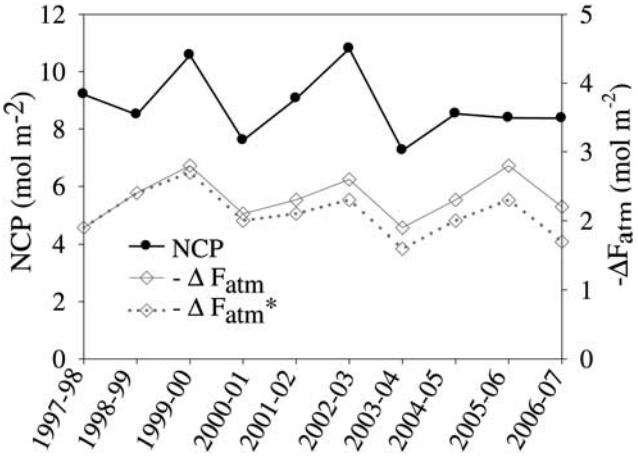

Fig. 4. Interannual variability of seasonal net community production (NCP) and ΔF_{atm} during the period 1997–2007. ΔF_{atm} was also calculated with fixed atmospheric fCO_2 concentration (363.2 ppm in 1998) and is called ΔF_{atm}*.

The timing of the second peak likewise displayed also large variability occurring from mid-December in 1999–2000 to mid-February in 1998–99. The most intense bloom was recorded in 2005–06 when chl *a* reached 4 and 2.35 mg m^{-3}, successively. This is more than 1.5 fold higher than in 1997–98, 1999–2000, 2003–04 and 2004–05.

The SST (1997–2007) variations are shown in Fig. 2b. Sea surface temperatures ranged from 1.4 ± 0.4°C in early October to 3.8 ± 0.4°C at the end of March. The coolest summer occurred in 1998–2000, and the warmest in 2001–04. While is it clear that chl *a* and SST displayed significant interanual variability, no clear decadal trends appeared (Fig. 2) as discussed for the Indian sector of the Southern Ocean by Metzl *et al.* (2006).

Results and discussion

Comparison of the Si(OH)$_4$ and DIC as well as fCO_2 simulations with field data over the 2005–08 period

The model was run using the chl *a*, SST (Fig. 2) and SSW over the 2005–08 period. Results were compared with the $Si(OH)_4$, DIC, fCO_2 measurements made in January 2006 and 2007 during the OISO cruises. Simulations on the date of the measurements and for the whole corresponding month (e.g. January) are shown in Table III.

The range of DIC and fCO_2 simulated in January 2007 agree well with the observations, while those simulated in January 2006 slightly (-5%) underestimate field data from January 2006. Most of the differences between the simulated and experimental concentrations were related with $Si(OH)_4$ concentrations. $Si(OH)_4$ concentrations in January 2006 were reproduced by the model while experimental $Si(OH)_4$ concentration was twofold higher in January 2007. Keeping in mind that the bloom was dominated by diatoms, this high

https://doi.org/10.1017/S0954102011000411 Published online by Cambridge University Press

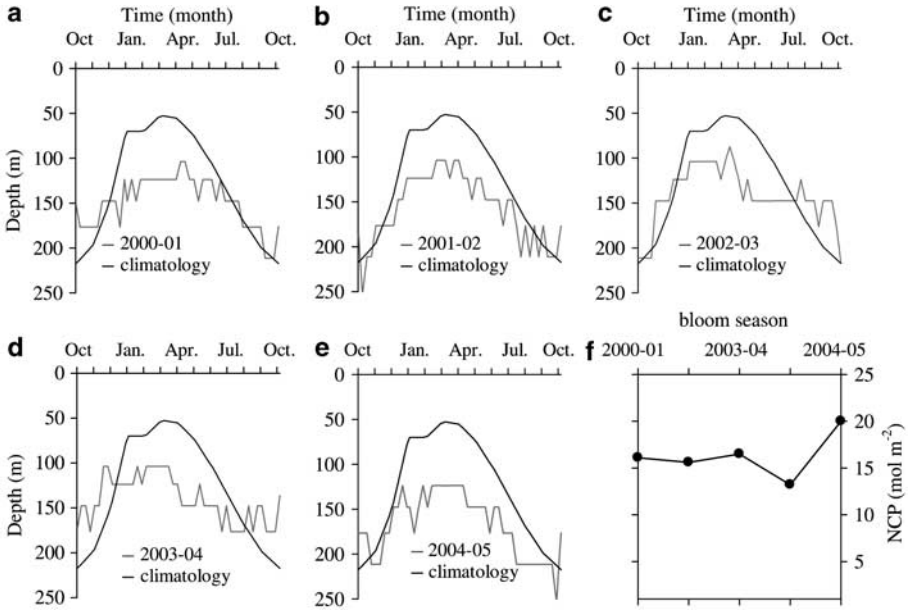

Fig. 5. a.–e. Evolution of the reference mixed layer depth (MLD) simulated using ROMS (grey line) for 2000–05. The reference MLD (from Metzl *et al*. (2006)) is shown (black line) for all seasons. **f.** The net community production (NCP) was computed using these ML and a new parametrization ($\mu_{max} = 1\ d^{-1}$).

$Si(OH)_4$ concentration was unexpected and could not be reproduced by the model.

In the carbonate system, the low interannual variability (relative standard deviation (rsd)) of the observed DIC (rsd = ± 0.3%) and fCO_2 (rsd = ± 1%) was reproduced by the model (rsd = ± 0.3%, rsd = ± 1%).

The simulated seasonal NCP was 8.4 mol m^{-2} for the seasons 2005–06 and 2006–07. The seasonal NCP were also calculated from a carbon budget (NCP_{cal}) according to the method described in Jouandet *et al*. (2008), using a MLD of 70 ± 20 m and $K_z = 3.10^{-4}\ m^2\ s^{-1}$ and DIC, $Si(OH)_4$ profiles taken during OISO cruises. NCP_{cal} were 6.3 ± 2.5 mol m^{-2} and 6.4 ± 2.6 mol m^{-2} for the 2005–06 and 2006–07 blooms, respectively. Simulated NCP were within the range of calculated NCP and were characterized by the same interannual variability. The model could then be used to investigate the interannual variability of NCP and ΔF_{atm} over longer periods.

Interannual variability of NCP and ΔF_{atm} during 1997–2007

The model was applied to explore the interannual variability of NCP and ΔF_{atm}, during the 1997–2007 period, using chl *a*, SST (Fig. 2) and SSW. The seasonal variation of the MLD from Metzl *et al*. (2006) was applied each year. This assumption is discussed later.

During the 1997–2007 period, the seasonal NCP varied between 7.3 mol m^{-2} (2003–04) and 10.8 mol m^{-2} (2002–03) with a mean value of 8.5 ± 1.2 mol m^{-2} (Fig. 4). The interannual variability of the NCP was low (rsd = ± 14%) compared with the interannual variability of the bloom magnitude (rsd = ± 88%). Moreover NCP maxima were not associated with bloom intensity maxima. For example, the NCP was lower in 2005–06 than in 1999–2000, while chl *a* peaks were twofold higher in 2005–06 than in 1999–2000 (Fig. 4, Table III). This comparison highlights the importance of the duration rather than the magnitude of the bloom. This may partly explain the high NCP in 1999–2000 and the low interannual variability of the NCP over the 1997–2007 decade. The highest NCP simulated in 1999–2000 may also result from the effect of the MLD on the calculation. The first chl *a* peak (leading to high $(\delta DIC/\delta t)_{bio}$) for the 1999–2000 bloom occurred in November when the mixed layer was deep, while the first chl *a* peak for the 2005–06 bloom (leading to high $(\delta DIC/\delta t)_{bio}$) occurred in January when the mixed layer was shallow (Table I, Fig. 3). Net community production was maximal for the earliest bloom because high $(\delta DIC/\delta t)_{bio}$

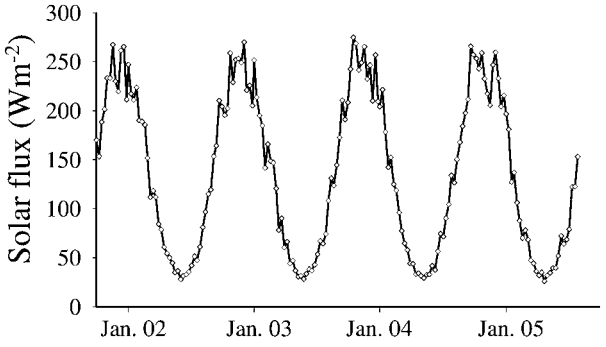

Fig. 6. Seasonal evolution of the solar flux for the 2001–05 period.

https://doi.org/10.1017/S0954102011000411 Published online by Cambridge University Press

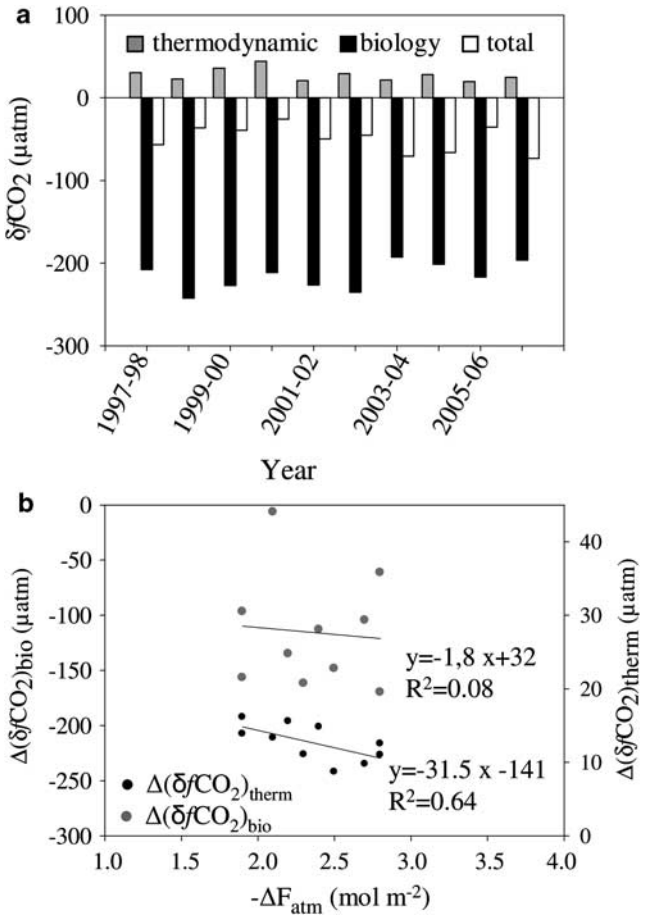

Fig. 7. a. Evolution of processes responsible for CO_2 fugacity (fCO_2) changes from the bloom season 1998–99 to 2006–07. **b.** ΔF_{atm} as a function of integrated fCO_2 changes due to the biological activity ($\Delta(fCO_2)_{bio}$) and temperature effect ($\Delta(\delta fCO_2)_{therm}$).

were associated with deep mixed layers. Nevertheless this hypothesis should be viewed with caution because the start of the bloom is expected to be dependant on the depth of the mixed layer.

The interplay between the start of the bloom and the MLD as well as the sensitivity of the model to the MLD were investigated using MLD simulated by the Regional Ocean Model system (ROMS) for the 2000–05 period (Fig. 5). The simulated MLD was deeper (+40 m) than the MLD from Metzl *et al*. (2006) and the MLD estimated during KEOPS. This difference was mainly due to the boundary conditions in the model derived from the coarse resolution Global Ocean Circulation Model OGCMs (Carton *et al*. 2005) which does not well represent the temperature minimum characteristic of waters south of the Polar Front accurately. The simulated MLD could only be used to investigate qualitatively the interannual variability of the NCP. The timing of the stratification of the ML in 2000–01, 2001–02 and 2004–05, was similar to that of the reference MLD cycle (MLD from Metzl *et al*. (2006)).

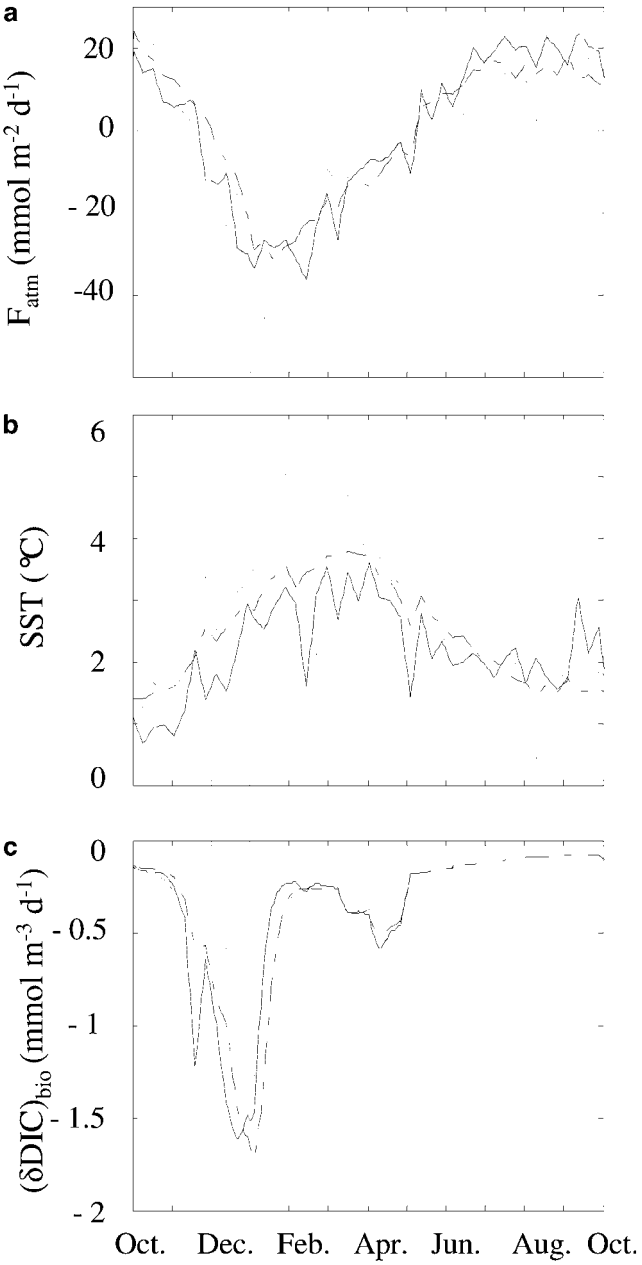

Fig. 8. Daily evolution of **a.** F_{atm}, **b.** sea surface temperature (SST), and **c.** biological consumption of dissolved inorganic carbon (DIC) for 1999–2000 and 2002–03. The climatology was computed as an average of all seasons.

But in 2002–03 an early bloom was observed and the stratification started earlier also. This observation argues against our proposed explanation that early blooms provide a large contribution to seasonal NCP due to a deep MLD. However, in 2003–04 earlier stratification did not correspond to an early bloom and no general trend could be drawn. The interannual variability of the solar radiation flux (http://www.esrl.noaa.gov/psd/cgi-bin/db_search/DBSearch.pl?Variable=Downward+Solar+Radiation+Flux&group=0&submit=Search, accessed October 2007) was investigated as an

https://doi.org/10.1017/S0954102011000411 Published online by Cambridge University Press

alternative explanation and is shown in Fig. 6. The low interannual variability of the flux did not explain the interannual variability of the start of the bloom either.

Therefore new field studies or improved modelling of the variability of the MLD above the Kerguelen plateau are needed to further address our hypothesis. Interestingly our conclusion that the interannual variability of seasonal NCP is low compared to the high interanual variability of the chl *a* remains valid when varying MLD annual cycles were used in the model (Fig. 5f).

The low interannual variability of simulated NCP could also result from parameterization of the model which does not take into account changes of the kinetics parameters due to shifts in structure of the phytoplankton community. A lack of data on the interannual variability of the phytoplankton community however does not allow us to overcome this limit.

During the 1997–2007 summers, this region acted as a net sink for atmospheric CO_2 with seasonal ΔF_{atm} values between -2.7 and -1.7 mol m^{-2} (Fig. 3). A large CO_2 uptake was observed for the highest NCP (i.e. 1999–2000 and 2002–03 blooms). At the seasonal scale ΔF_{atm} was better correlated with the biological effect rather than thermodynamic effect (Fig. 7b). By contrast, over an interannual timescale most of the ΔF_{atm} variability results from the interannual variability of $\Delta(\delta fCO_2)$ due to temperature changes $(\Delta(\delta fCO_2)_{therm})$ (Fig. 7a). The comparison between the blooms of 1999–2000 and 2002–03 illustrate this pattern.

The effect of air-sea CO_2 solubility on ΔF_{atm} is demonstrated when comparing F_{atm} simulated in 1999–2000 with F_{atm} simulated in 2002–03 while keeping the atmospheric CO_2 at a constant xCO_2 of 363.2 ppm in 1998 (Fig. 8). Bloom characteristics (i.e. duration, timing and magnitude) were similar for both seasons allowing the separation of the SST effect from the biological effect on the ΔF_{atm} flux. ΔF_{atm} and $(\delta DIC)_{bio}$ integrated from the start of the bloom to the end of January were similar for both years (1.5 mol m^{-2} and 78 mmol m^{-3} respectively) while SST was higher in 2002–03 (Fig. 8). This comparison highlights the control of F_{atm} by the biological activity during this period. By contrast, large difference of F_{atm} was simulated during the decline of the bloom (from February–April), due to the effect of solubility. Sea surface temperatures were higher (up to 1.7°C) in 2002–03 than in 1999–2000, leading to a higher fCO_2 in the mixed layer and a F_{atm} 16% lower in 2002–03. This scenario emphasizes the role of temperature as the fundamental factor controlling the air-sea CO_2 exchanges at the seasonal scale, in this productive area.

Conclusion

Our analysis of the interannual variability of the Kerguelen plateau bloom emphasizes the possible importance of the duration and the early start of the bloom in controlling the magnitude of the seasonal NCP. This is a key result as sea surface warming, stratification and duration of the blooms are expected to change in the future as a consequence of climate change (Bopp *et al*. 2001). Previous studies in typical HNLC waters of the Permanent Open Ocean Zone have shown that when the ocean is warmer, biological activity dominates the thermodynamic effect leading to a stronger summer ocean CO_2 sink (Jabaud-Jan *et al*. 2004, Brévière *et al*. 2006). By contrast, our analysis conducted in the highly productive region of the Kerguelen plateau, shows that the CO_2 sink is governed by a complex interplay of thermodynamics and biological activity and presents relatively low variability over ten years. Given the high variability of the chl *a* maximum in the Kerguelen plateau region the small changes in NCP and air-sea CO_2 fluxes were not expected. These results highlight the importance of investigating in more detail the coupling between warming/cooling and biological activity in order to better evaluate the impact of climate change on the Southern Ocean CO_2 sink.

Acknowledgements

Thanks to the Kerguelen Ocean and Plateau Compared Study (KEOPS) and the Ocean Indian Service Observation (OISO) shipboard science team and the officers and crew of RV *Marion Dufresne* for their efforts. The OISO program is supported by INSU, IPEV and Institut Pierre Simon Laplace (IPSL). We also thank two anonymous referees for their valuable comments.

References

Bates, N.R., Hansell, D.A., Carlson, C.A. & Gordo, L.I. 1998. Distribution of CO_2 species, estimates of net community production, and air-sea CO_2 exchange in the Ross Sea polynya. *Journal of Geophysical Research*, **103**, 2883–2896.

Blain, S., Quéguiner, B., Armand, L., Belviso, S., Bombled, B., Bopp, L., Bowie, A., Brunet, C., Brusaard, C., Carlotti, F., Christaki, U., Corbière, A., Durand, I., Ebersbach, F., Fuda, J.-L., Garcia, N., Gerringa, L., Griffiths, B., Guigue, C., Guillerm, C., Jacquet, S., Jeandel, C., Laan, P., Lefèvre, D., Monaco, C., Malits, A., Mosseri, J., Obernosterer, I., Park, Y.-H., Picheral, M., Pondaven, P., Remenyi, T., Sandroni, V., Thuiller, D., Timmermans, K., Trull, T., Uitz, J., van Beek, P., Veldhuis, M., Vincent, D., Viollier, E., Vong, L. & Wagener, T. 2007. Impacts of natural iron fertilization on the Southern Ocean. *Nature*, **446**, 1070–1074.

Bopp, L., Monfray, P., Aumont, O., Dufresne, J.L., Le Treut, H., Madec, G., Terray, L. & Orr, J.C. 2001. Potential impact of climate change on marine export production. *Global Biogeochemical Cycles*, **15**, 81–99.

Brévière, E., Metzl, N., Poisson, A. & Tilbrook, B. 2006. Changes of the oceanic CO_2 sink in the Eastern Indian sector of the Southern Ocean. *Tellus*, **58B**, 438–446.

Brzezinski, M.A. 1985. The Si:C:N ratio of marine diatoms: interspecific variability and the effect of some environmental variables. *Journal of Phycology*, **21**, 347–357.

Carton, J.A., Giese, B.S. & Grodsky, S.A. 2005. Sea level rise and the warming of the oceans in the Simple Ocean Data Assimilation (SODA) ocean reanalysis. *Journal of Geophysical Research*, **110**, 10.1029/2004JC002817.

CASSAR, N., BENDER, M.L., BARNETT, B.A., FAN, S., MOXIM, W.J., LEVY II, H. & TILBROOK, B. 2007. The Southern Ocean biological response to aeolian iron deposition. *Science*, **317**, 1067–1070.

FASHAM, M.J.R., FLYNN, K.J., PONDAVEN, P., ANDERSON, T.R. & BOYD, P. 2006. Development of a robust marine ecosystem model to predict the role of iron in biogeochemical cycles: a comparison of results for iron-replete and iron-limited areas, and the SOIREE iron-enrichment experiment. *Deep-Sea Research I*, **53**, 333–366.

HO, D.T., LAW, C.S., SMITH, M.J., SCHLOSSER, P., HARVEY, M. & HILL, P. 2006. Measurements of air-sea gas exchange at high wind speeds in the Southern Ocean: implications for global parameterizations. *Geophysical Research Letters*, **33**, 10.1029/2006GL026817.

HOPPEMA, M., MIDDAG, R., DE BAAR, H.J.W., FAHRBACH, E., VAN WEERLEE, H. & THOMAS, E.M. 2007. Whole season net community production in the Weddell Sea. *Polar Biology*, **31**, 101–111.

ISHII, M., INOUE, H.Y. & MATSUEDA, H. 2002. Net community production in the marginal ice zone and its importance for the variability of the oceanic pCO_2 in the Southern Ocean south of Australia. *Deep-Sea Research II*, **49**, 1691–1706.

ISHII, M., INOUE, H.Y., MATSUEDA, H. & TANOUE, E. 1998. Close coupling between seasonal biological production and dynamics of dissolved inorganic carbon in the Indian Ocean sector and the western Pacific Ocean sector of the Southern Ocean. *Deep-Sea Research I*, **45**, 1187–1209.

JABAUD-JAN, A., METZL, N., BRUNET, C., POISSON, A. & SCHAUER, B. 2004. Interannual variability of the carbon dioxide system in the Southern Indian Ocean (20°S–60°S): the impact of a warm anomaly in austral summer 1998. *Global Biogeochemical Cycles*, **18**, 1–20.

JOUANDET, M.P., BLAIN, S., METZL, N., TRULL, T.W. & OBERNOSTERER, I. 2008. A seasonal carbon budget for a naturally iron fertilized bloom over the Kerguelen plateau in the Southern Ocean. *Deep-Sea Research II*, **55**, 856–867.

KARL, D.M., TILBROOK, B.D. & TIEN, G. 1991. Seasonal coupling of organic matter production and particule flux in the western Brandsfield Strait, Antartica. *Deep-Sea Research II*, **38**, 1097–1126.

LOUANCHI, F., METZL, N. & POISSON, A. 1996. Modeling the monthly sea surface pCO_2 fields in the Indian Ocean. *Marine Chemistry*, **55**, 265–279.

METZL, N. 2009. Decadal increase of ocean carbon dioxide in the southern Indian Ocean surface waters (1991–2007). *Deep-Sea Research II*, **56**, 607–619.

METZL, N., BRUNET, C., JABAUD-JAN, A., POISSON, A. & SCHAUER, B. 2006. Summer and winter air-sea CO_2 fluxes in the Southern Ocean. *Deep-Sea Research I*, **53**, 1548–1563.

MOORE, J.K. & ABBOTT, M.R. 2002. Surface chlorophyll concentrations in relation to the Antarctic Polar Front: seasonal and spatial patterns from satellite observations. *Journal of Marine System*, **37**, 69–86.

MOSSERI, J., QUEGUINER, B., ARMAND, L. & CORNET-BARTHAU, V. 2008. Impact of iron on silicon utilization by diatoms in the Southern Ocean: a case of Si/N cycle decoupling in a naturally iron-enriched area. *Deep-Sea Research II*, **55**, 801–819.

NIGHTINGALE, P.D., MALIN, G., LAW, C.S., WATSON, A.J., LISS, P.S., LIDDICOAT, M.I., BOUTIN, J. & UPSTILL-GODDAD, R.C. 2000. In-situ elevation of air sea gas exchange parametrizations using novel conservative and volatile tracers. *Global Biogeochemical Cycles*, **14**, 373–387.

OBERNOSTERER, I., CHRISTAKI, U., LEFEVRE, D., CATALA, P., VAN WAMBEKE, F. & LEBARON, P. 2008. Rapid bacterial mineralization of organic carbon produced during a phytoplankton bloom induced by natural iron fertilization in the Southern Ocean. *Deep-Sea Research II*, **55**, 777–789.

PONDAVEN, P., RUIZ-PINO, D., FRAVALO, C., TREGUER, P. & JEANDEL, C. 2000. Interannual variability of Si and N cycles at the time-series station KERFIX between 1990 and 1995 - a 1-D modelling study. *Deep-Sea Research I*, **47**, 223–257.

RUBIN, S.I., TAKAHASHI, T., CHIPMAN, D.W. & GODDARD, J.G. 1998. Primary productivity and nutrient utilization ratios in the Pacific sector of the Southern Ocean based on seasonal changes in seawater chemistry. *Deep-Sea Research II*, **45**, 1211–1234.

SULLIVAN, C.W., ARRIGO, K.R., MCCLAIN, C.R., COMISO, J.C. & FIRESTONE, J. 1993. Distributions of phytoplankton blooms in the Southern Ocean. *Science*, **262**, 1832–1837.

SWEENEY, C., SMITH, W.O., HALES, B., BIDIGARE, R., CARLSON, C.A., CODISPOTI, L.A., GORDON, L.I., HANSELL, D.A., MILLERO, F.J., PARK, M.-O.K. & TAKASHI, T. 2000. Nutrient and carbon removal ratios and fluxes in the Ross Sea, Antarctica. *Deep-Sea Research II*, **47**, 3395–3421.

TYRRELL, T., MERICO, A., WANIEK, J.J., WONG, C.S., METZL, N. & WHITNEY, F. 2005. Effect of seafloor depth on phytoplankton blooms in high-nitrate, low-chlorophyll (HNLC) regions. *Journal of Geophysical Research*, **110**, 1–12.

WANNINKHOF, R. 1992. Relationship between wind speed and gas exchange over the ocean. *Journal of Geophysical Research*, **97**, 7373–7382.

WEISS, R.F. 1974. Carbon dioxide in water and seawater: the solubility of a non-ideal gas. *Marine Chemistry*, **8**, 347–359.